Published in final edited form as:
FEBS Lett. 2013 May 2; 587(9): 1304–1309. doi:10.1016/j.febslet.2013.02.033.

Functional differences between *Streptococcus pyogenes* cluster 1 and cluster 2b streptokinases are determined by their β-domains

Yueling Zhang, **Zhong Liang**, **Kristofor Glinton**, **Victoria A. Ploplis**, and **Francis J. Castellino***
W.M. Keck Center for Transgene Research and Department of Chemistry and Biochemistry, University of Notre Dame, Notre Dame, IN 46556, USA

Abstract

Cluster 1 streptokinases (SK1) from *Streptococcus pyogenes* (GAS) show substantially higher human plasminogen (hPg) activation activities and tighter hPg binding affinities than cluster 2b streptokinases (SK2b) in solution. The extent to which the different domains of SK are responsible for these differences is unknown. We exchanged each of the three known SK domains (α, β, and γ) between SK1 and SK2b and assessed the function of the resulting variants. Our results show that primary structural differences in the β-domains dictate these functional differences. This first report on the primary structure–functional relationship between naturally occurring SK1 and SK2b sheds new light on the mechanism of hPg activation by SK, a critical virulence determinant in this species of human pathogenic bacteria.

Keywords

Streptokinase; Fibrinolysis; Protein domains; Virulence; *Streptococcus pyogenes*

1. Introduction

Plasminogen (hPg), a soluble plasma 791-residue single-chain glycoprotein, is the zymogen form of the serine protease, plasmin (hPm), a major component of the mammalian fibrinolytic system. In humans, hPg is activated to hPm as a result of cleavage of a single peptide bond, Arg^{561}–Val^{562} in hPg, thus forming the disulfide-linked two-chain, hPm [1]. Mammalian hPg activators, *e.g.*, urokinase-type plasminogen activator (uPA) and tissue-type plasminogen activator (tPA), are themselves serine proteases with exquisite specificity for hPg activation. On the other hand, one critical and highly specific activator of hPg, *viz.*, streptokinase (SK), secreted by several *streptococcal* strains, including the human pathogen, *Streptococcus pyogenes* (GAS), is a single-chain protein of 414 amino acids [2]. This protein forms a line of communication between the bacterium and the human host for establishing a proteolytic environment for GAS, a feature that greatly enhances its invasive properties [3]. One unique feature of SK is that it is not a protease, and the manner in which it activates hPg through a series of protein–protein complexes, has been a subject of detailed study [4].

* Corresponding author. Fax: +1 574 631 8017. fcastell@nd.edu. .

Appendix A. Supplementary data Supplementary data associated with this article can be found, in the online version, at http://dx.doi.org/10.1016/j.febslet.2013.02.033.

Until recently, nearly all mechanistic studies of hPg activation by SK were performed with SKg, a SK from *Streptococcus dysgalactiae* subsp. *equismilis*, which has been widely used in humans to dissolve fibrin-containing thrombi that cause myocardial infarctions [5,6]. The X-ray crystal structure of SKg bound to the catalytic domain of human plasmin (hPm) shows that SK consists of three similar "β-grasp-folding" domains (α, β, and γ domains), separated by two flexible loops. These three domains bind to the isolated hPm catalytic domain and form a "three-sided crater" around the hPm active site [7].

Numerous studies have been aimed at elucidating the function of each SK domain in hPg/hPm binding and activation. Various SK variants, including single and multiple domain constructs and point mutations [8–19], have been generated to attempt to clarify the functions of each of the SK domains in hPg binding and activation. Collectively, these studies generated a complex mixture of functional effects leading to a variety of different conclusions, but all of these studies agreed that there is some level of cooperation between the domains in hPg activation.

While many of these investigations relied on mutagenic changes in one strain of SK, SKg, other opportunities have arisen from findings that natural SKs from different GAS strains show considerable sequence variability, especially in their β-domains [20,21]. From the diversity of these primary structures, SKs from GAS were classified into two clusters, cluster 1 (SK1) and cluster 2 (SK2). Based on sequence analyses, cluster 2 was further subdivided into cluster 2a (SK2a) and 2b (SK2b) [20]. Recent data obtained on SK1 and SK2b demonstrated that their properties toward hPg binding and activation were very different [3,21], thus allowing natural mutants for SK structure–function studies to be examined. In this regard, exchange of a partial β domain (residues 124–238) between SKs from GAS strains NZ131 and SF13013 has been performed, but did not uncover any effects on hPg activation kinetics [22]. In retrospect, this result would be expected since the two SKs, themselves, show similar hPg activation functions, despite the fact that the two regions exchanged share less than 50% identity.

This variety of available natural SK variants offers rational mutagenesis strategies to study the structure–function relationships of SK. Exchange of domains between cluster 1 and cluster 2b SKs have been performed, and the resulting hPg binding and activation activity changes are revealed in the current study.

2. Materials and methods

2.1. cDNAs and proteins

DNA sequences of cluster 1 sk (sk1) clones, sk_{NS210}, sk_{NS53}, sk_{NS931}, sk_{NZ131}, and cluster 2b sk (sk2b) clones, sk_{AP53}, sk_{NS223}, sk_{NS455} and $sk_{NS88.2}$, have been described in a previous study [21]. Among this group, sk_{NS931} and $sk_{NS88.2}$ were employed as prototypical wild-type (WT) sk1 and sk2b, respectively. These genes were assembled into plasmid pET42a (EMD4 Biosciences, Germany) [21] for gene mutagenesis and protein expression.

Human full-length Glu^{1}-plasminogen (hPg), and its latent hPm active-site mutant, hPg [$S^{741}A$], were expressed in *Drosophila* Schneider S2 cells and purified as described [21,23].

2.2. Construction, expression and purification of SK mutants

PCR-mediated overlap-extension was used to construct SK mutant expression plasmids [24]. The primers used are listed in Supplementary Table 1 and the strategy of their use to construct the variants is shown in Supplementary Table 2. The resulting constructions contained the coding sequences for 414 amino acid residues of rSK variants, placed between restriction sites PshAI and BamHI of pET42a (EMD4Biosciences, Germany). For

expression, *Escherichia coli* BL21(DE3) cells (New England Biolabs, USA) were transformed with the pET42a constructs. Importantly, all rSKs generated were designed to contain their natural amino-terminal amino acid [25].

The SK variant proteins were expressed and purified as described [21]. The purity of all rSK mutants was assessed with 12% SDS–PAGE. Protein concentrations were measured at A_{280nm} using the calculated (Protein Calculator, version 3.3) extinction coefficients (M^{-1} cm^{-1}): rSK_{M1}, 35130; rSK_{M2}, 31290; rSK_{M3}, 33850; rSK_{M4}, 32570; rSK_{M5}, 32570; rSK_{M6}, 33850.

2.3. Circular dichroism (CD) measurements

CD spectra were collected between 190–240 nm using an AVIV 202SF spectrometer (Lakewood, NJ). Spectral scans were obtained at 25 °C at 0.2 nm intervals at a rate of 60 nm/min, in a 0.1 cm quartz cuvette. Three runs were averaged for each sample. A buffer reference scan was subtracted from the sample scans. The mean residue elipticities (MRE) were calculated using the equation, MRE = ($\theta \times$ MRW)/(1 × c), where θ is the CD signal in millidegrees, MRW is the mean residue weight in g/mol, l is the path length in millimeters and c is the protein concentration in mg/ml.

2.4. Activation of Glu^1-hPg

HPg activation rates were monitored in 96-well microtiter plates in Cl^- buffer to maintain the closed (tight) conformation of hPg [26,27]. The activation of hPg was accelerated by the addition of catalytic levels of rSK as detailed earlier [21]. The amidolytic activity of the generated plasmin (hPm) was continuously monitored by the absorbance (A) at 405 nm from release by plasminolysis of pnitroanilide (pNA) from the chromogenic substrate, S2251 (H-D-Val-Leu-Lys-pNA; Chromogenix, Italy). Because, under these conditions, the A_{405nm} reflects hPm activity from continually increasing [hPm], for more quantitative estimates the A_{405nm} was also plotted against t^2 [28]. The initial velocities were then calculated from the slopes of the linear regions of these plots. All data transformations and linear regressions were performed using GraphPad Prism 5.

2.5. Surface plasmon resonance (SPR)

K_d values of hPg binding to SK were measured by SPR with a BIAcore X100 (GE Healthcare) from association (k_{on}) and dissociation (k_{off}) rates. A hPg mutant, rhPg[$S^{741}A$], in which the latent active-site, Ser^{741}, was replaced with Ala, was used to avoid hPm production during the binding process. Our procedural details have been described [21].

3. Results and discussion

3.1. Conservation and diversity between SK1 and SK2b

Previous studies have revealed that SK1 and SK2b showed significant differences in binding to, and activation of, hPg [3,21,29]. SK1 displays a > 10-fold tighter binding affinity, and a correspondingly higher activation activity toward hPg than SK2b [21]. To explore the primary structural features of SK that are responsible for these differences, the amino acid sequences of four SK1s and four SK2bs from various GAS strains [21] were compared (Fig. 1A). The α- and γ-domains showed higher conservation (77% and 84% identity, respectively) than the β-domains (55% identity) among all these SKs (asterisked, Fig. 1A). This is consistent with the finding that the SK β-domain displays the highest level of sequence heterogeneity [20]. When those diverse residues (unasterisked, Fig. 1A) were investigated, a number of residues (boxed in Fig. 1A) were found to be conserved in the SK1 cluster, but were different between the SK1 and SK2b clusters.

Although a larger proportion (53%) of these cluster-conserved residues appeared in the β-domain, they were also found in the α- and γ-domains (30% and 17%, respectively). This indicates that all three domains are potential determinants for the functional differences between SK1 and SK2b. In addition, from the results obtained with SKg, all three domains have been suggested to play roles in both hPg binding and activation [12,16,18,30,31]. However, information provided to this time does not yield sufficient information to confirm which domain or domains plays a determinate role in hPg activation.

3.2. Expression, purification, and secondary structural analysis of SK mutants

SK contains three independent functional domains, separated by flexible loops, with no direct interaction between domains [30]. Thus, it is plausible that swapping one domain between two SKs will not affect the functions of the other two, and/or that the new domain introduced will display functions attributed to its parent SK.

To further determine which domain or domains plays the determinate role in the large functional differences between SK1 and SK2b, one SK from each cluster was selected for domain-swapping investigations, *viz.*, SKs from GAS strains NS931 ($SK1_{NS931}$) and NS88.2 ($SK2b_{NS88.2}$), respectively. Six mutants, SK_{M1} through SK_{M6}, were then constructed by exchanging each of the three domains between WT-$SK1_{NS931}$ and WT-$SK2b_{NS88.2}$, as illustrated in the scheme of Fig. 1B. The mutants were expressed in *E. coli* BL21(DE3) and purified as described [21]. Final yields were 8–12 mg protein/l culture, and SDS–PAGE (Fig. 2) showed that these mutants display >95% purity and appear in the expected calculated size range (44–49 kDa).

Far-UV circular dichroism (CD) spectroscopy was employed to compare the secondary structures of these rSK mutants with WT-$rSK1_{NS931}$ and WT-$rSK2b_{NS88.2}$. As shown (Fig. 3), despite the domain diversities, the purified rSK domain-exchanged mutants showed very similar CD spectra to those of the WT-rSKs throughout the wavelength range of 192–240 nm. The output spectra obtained were typical of those expected for a combination of α helical (minima at 208 and 222 nm, maxima at 190 nm) and β-sheet (minima at 218 nm, maxima at 196 nm), indicative of the known structure of SK [30]. When the CD spectra of all WT and mutant SK's were analyzed with an online CD structural algorithm (http://geneura.ugr.es/cgi-bin/somcd/som.cgi?start=1), the α-helical content ranged from 12–20%, the β-sheets from 35–40%, the β-turn content from 9–12%, and random structures from 29–38%; all within experimental uncertainty of the method. Thus, these high similarities in the rSK mutants with WT-rSKs indicates that swapping of domains does not substantially affect the gross structures of SKs.

3.3. The α- and γ-domains play minor roles in the hPg activation differences between SK1 and SK2b

SK1 activates hPg at a much higher rate than that of SK2b [3,20]. To study whether such an important property resides within specific domains of SK1, the corresponding hPg-activation activities of the above-purified domain-exchanged mutants were measured and compared to those of the WT-SKs. As shown (Fig. 4A and B), when the $SK1_{NS931}$ α-domain (α_1) was replaced by the α-domain from $SK2b_{NS88.2}$ (α_{2b}), the hPg activation rate in solution by the resulting rSK_{M1} ($\alpha_{2b}\beta_1\gamma_1$), of 0.43 mA_{405nm}/min^2, was somewhat attenuated from that of WT-$SK1_{NS931}$ ($\alpha_1\beta_1\gamma_1$), which was determined to be 1.08 mA_{405nm}/min^2. However, the increase in hPg activation rate by rSK_{M1} is still much faster, by ~13-fold, than that of $rSK2b_{NS88.2}$ ($\alpha_{2b}\beta_{2b}\gamma_{2b}$) and rSK_{M2} ($\alpha_1\beta_{2b}\gamma_{2b}$).

Similarly, exchange of the γ_1 domain for γ_{2b} in $rSK2b_{NS88.2}$, providing mutant rSK_{M6} ($\alpha_{2b}\beta_{2b}\gamma_1$), did not enhance the very low hPg activation activity of $rSK2b_{NS88.2}$, and

exchange of γ_{2b} with γ_1 in rSK_{NS931}, yielding rSK_{M5} ($\alpha_1\beta_1\gamma_{2b}$), attenuated the activation rate by approximately one-half of that of WT-$rSK1_{NS931}$ (Fig. 4A and B). These slightly diminished activation rates suggest minor roles for the α- and γ-domains in enhancing activation of hPg by SK1 in solution, but the overall similar activation rates of the mutants as those of their parental WT-SKs indicated that neither the α-domain nor the γ-domain is a determinant of the activity differences between SK1 and SK2b.

3.4. The β-domain plays a pivotal role in the hPg activation differences between SK1 and SK2b

More dramatic effects are noted in SK activation of hPg when considering the SK β-domains. Introduction of β_{2b} in place of β_1 in $rSK1_{NS931}$, yielding variant rSK_{M3} ($\alpha_1\beta_{2b}\gamma_1$), resulted in a 35-fold reduction of activity from WT-$rSK1_{NS931}$, which was actually equal to that of $rSK2b_{NS88.2}$ (Fig. 4A and B), while the replacement of β_{2b} by β_1, providing variant rSK_{M4} ($\alpha_{2b}\beta_1\gamma_{2b}$), enhanced the hPg activation activity in solution by ~12-fold (Fig. 4A and B). Clearly, the β-domain plays an important functional role in the ability of SK1 to activate hPg.

Thus, whereas the β1 region is by-far the most important domain for the high activity of SK1 compared to SK2b, the α_1 and γ1 domains assist, probably in a synergistic fashion, in achieving the high activation rates seen in WT-SK1, compared to WT-SK2b, as can be seen in the variants with the α_1 or γ_1 domains replaced by α_{2b} or γ_{2b}, in which the activation rates of SK1 decreased 55% in rSK_{M1} and 42% in rSK_{M5}.

3.5. β-Domain exchanges lead to large changes in binding affinities of SK to hPg

Another significant functional difference between SK1 and SK2b is that SK1 shows a >10-fold higher affinity to hPg than SK2b, as typified by WT-$rSK1_{NS931}$ and WT-$rSK2b_{NS88.2}$ (Table 1). This overall finding is in-keeping with the more rapid activation of hPg in solution by SK1 [3,21]. To study whether individual domains of SK1 and SK2b independently determine the affinities of SK1 and SK2b to hPg, SPR was used to investigate the binding energies of the SK mutants to hPg. Some example sensorgrams are shown inFig. 5 and the K_d values are listed in Table 1.

Compared to WT-$rSK1_{NS931}$ ($\alpha_1\beta_1\gamma_1$), the introduction of α_{2b} into SK1 in place of α_1, in the variant rSK_{M1} ($\alpha_{2b}\beta_1\gamma_1$), results in a very small effect on the K_d (Table 1), as is the case when the γ_1 domain is replaced by γ_{2b} in variant rSK_{M5} ($\alpha_1\beta_1\gamma_{2b}$). In neither case was the K_d increased by >twofold. These binding data, similar to the results of the activation kinetics, suggest that the α_1 and γ_1 domains do not contribute substantially to the different binding affinities SK1 and SK2b to hPg. However, introduction of β_{2b} for β_1 in SK_{NS931} led to ~10-fold weaker affinity of rSK_{M3} ($\alpha_1\beta_{2b}\gamma_1$) as compared to WT-$rSK1_{NS931}$, brought the binding properties of rSK_{M3} closer to WT-$rSK2b_{NS88.2}$ as a result of this single β-domain exchange. These data demonstrate that the tighter binding affinity and corresponding higher activation rates of WT-$rSK1_{NS931}$, as compared to WT-$rSK2b_{NS88.2}$, is primarily determined by β-domain differences.

Other domain exchanges between $SK1_{NS931}$ and $SK2b_{NS88.2}$ (Table 1) allow similar conclusions to be reached. Specifically, replacement of the α_{2b} and γ_{2b} domains of $rSK2b_{NS88.2}$ ($\alpha_{2b}\beta_{2b}\gamma_{2b}$) with α_1 and γ_1 from $rSK1_{NS931}$, providing variants rSK_{M2} ($\alpha_1\gamma_{2b}\gamma_{2b}$) and rSK_{M6} ($\alpha_{2b}\beta_{2b}\gamma_1$), did lead to an ~3-fold enhancement in binding affinity in the case of rSK_{M2}, compared to WT-$rSK2b_{NS88.2}$, but still fivefold weaker than WT-$rSK1_{NS931}$. In the case of rSK_{M6} (Table 1), the γ_1 domain substitution did not affect its binding energy to rhPg[S^{741}A], when compared to $rSK_{NS88.2}$. However, exchange of the β_1-domain for β_{2b}, yielding variant rSK_{M4} (α1β2bγ1), showed an 18-fold higher affinity to

rhPg[S^{741}A] than WT-rSK2b$_{NS88.2}$, a value nearly the same as WT-rSK1$_{NS931}$. On the whole, the changes of affinities to hPg are consistent with the changes of hPg activation activities and demonstrate the critical role of the β-domain of SK, with synergy provided by the α-domain, in dictating the nature of its hPg activation activity specificity.

3.6. Conclusion and future prospects

The mutational and functional analyses provided in this study have revealed that the primary structural differences in the β-domain of SK is a major determinant of the important functional differences of SK1 and SK2b toward hPg activation. This largely narrows the range for other mutations to generate to assess the diverse functional properties of SKs produced by GAS strains with distinct tissue tropism and virulence. Since host hPm is a critical virulence determinant in this human pathogenic bacterium, understanding the nature of its activation in GAS is a very important goal in developing methods to attenuate the effects of GAS in humans.

Supplementary Material

Refer to Web version on PubMed Central for supplementary material.

Acknowledgments

This work was supported by National Institutes of Health Grant HL013423.

References

[1]. Castellino, FJ. Plasminogen in: Molecular Basis of Thrombosis and Hemostasis. High, KA.; Roberts, HR., editors. Marcel Dekker Inc.; New York, NY: 1995. p. 495-515.

[2]. Castellino, FJ.; Ploplis, VA. Plasminogen Structure, Activation, and Regulation Kluwer. Academic/Plenum Publishers; 2003. Human plasminogen: Structure, Activation, and Function; p. 3-17.

[3]. Cook SM, Skora A, Gillen CM, Walker MJ, McArthur JD. Streptokinase variants from *Streptococcus pyogenes* isolates display altered plasminogen activation characteristics – implications for pathogenesis. Mol. Microbiol. 2012; 86:1052–1062. [PubMed: 23106864]

[4]. Castellino, FJ.; Ploplis, VA. Plasminogen and streptokinase. In: Bachmann, F., editor. Handbook of Pharmacology. Vol. vol. 146. Springer-Verlag; 2001. p. 25-56.

[5]. Anderson JL, et al. A randomized trial of intracoronary streptokinase in the treatment of acute myocardial infarction. N. Engl. J. Med. 1983; 308:1312–1318. [PubMed: 6341843]

[6]. Hoffmeister HM, et al. Thrombolytic therapy in acute myocardial infarction – comparison of procoagulant effects of streptokinase and alteplase regimens with focus on the kallikrein system and plasmin. Circulation. 1998; 98:2527–2533. [PubMed: 9843458]

[7]. Boffa MB, Wang W, Bajzar L, Nesheim ME. Plasma and recombinant thrombin-activable fibrinolysis inhibitor (TAFI) and activated TAFI compared with respect to glycosylation, thrombin/thrombomodulin-dependent activation, thermal stability, and enzymatic properties. J. Biol. Chem. 1998; 273:2127–2135. [PubMed: 9442053]

[8]. Rodriguez P, et al. The streptokinase domain responsible for plasminogen binding. Fibrinolysis. 1994; 8:276–285.

[9]. Lin LF, Oeun S, Houng A, Reed GL. Mutation of lysines in a plasminogen binding region of streptokinase identifies residues important for generating a functional activator complex. Biochemistry. 1996; 35:16879–16885. [PubMed: 8988027]

[10]. Conejero-Lara F, Parrado J, Azuaga AI, Dobson CM, Ponting CP. Analysis of the interactions between streptokinase domains and human plasminogen. Protein Sci. 1998; 7:2190–2199. [PubMed: 9792107]

[11]. Chaudhary A, Vasudha S, Rajagopal K, Komath SS, Garg N, Yadav M, Mande SC, Sahni G. Function of the central domain of streptokinase in substrate plasminogen docking and processing revealed by site-directed mutagenesis. Protein Sci. 1999; 8:2791–2805. [PubMed: 10631997]

[12]. Loy JA, Lin X, Schenone M, Castellino FJ, Zhang XC, Tang J. Domain interactions between streptokinase and human plasminogen. Biochemistry. 2001; 40:14686–14695. [PubMed: 11724583]

[13]. Wu DH, Shi GY, Chuang WJ, Hsu JM, Young KC, Chang CW, Wu HL. Coiled coil region of streptokinase gamma-domain is essential for plasminogen activation. J. Biol. Chem. 2001; 276:15025–15033. [PubMed: 11278293]

[14]. Kim DM, Lee SJ, Yoon SK, Byun SM. Specificity role of the streptokinase C-terminal domain in plasminogen activation. Biochem. Biophys. Res. Commun. 2002; 290:585–588. [PubMed: 11779212]

[15]. Wakeham N, Terzyan S, Zhai P, Loy JA, Tang J, Zhang XC. Effects of deletion of streptokinase residues 48–59 on plasminogen activation. Protein Eng. 2002; 15:753–761. [PubMed: 12456874]

[16]. Sundram V, Nanda JS, Rajagopal K, Dhar J, Chaudhary A, Sahni G. Domain truncation studies reveal that the streptokinase–plasmin activator complex utilizes long range protein–protein interactions with macromolecular substrate to maximize catalytic turnover. J. Biol. Chem. 2003; 278:30569–30577. [PubMed: 12773528]

[17]. Bean RR, Verhamme IM, Bock PE. Role of the streptokinase alpha-domain in the interactions of streptokinase with plasminogen and plasmin. J. Biol. Chem. 2005; 280:7504–7510. [PubMed: 15623524]

[18]. Yadav S, Datt M, Singh B, Sahni G. Role of the 88–97 loop in plasminogen activation by streptokinase probed through site-specific mutagenesis. Biochim. Biophys. Acta. 2008; 1784:1310–1318. [PubMed: 18590837]

[19]. Yadav S, Aneja R, Kumar P, Datt M, Sinha S, Sahni G. Identification through combinatorial random and rational mutagenesis of a substrate-interacting exosite in the gamma domain of streptokinase. J. Biol. Chem. 2011; 286:6458–6469. [PubMed: 21169351]

[20]. Kalia A, Bessen DE. Natural selection and evolution of streptococcal virulence genes involved in tissue-specific adaptations. J. Bacteriol. 2004; 186:110–121. [PubMed: 14679231]

[21]. Zhang Y, Liang Z, Hsueh HT, Ploplis VA, Castellino FJ. Characterization of streptokinases from Group A *Streptococci* reveals a strong functional relationship that supports the coinheritance of plasminogen-binding M-Protein and cluster 2b streptokinase. J. Biol. Chem. 2012; 287:42093–42103. [PubMed: 23086939]

[22]. Lizano S, Johnston KH. Structural diversity of streptokinase and activation of human plasminogen. Infect. Immun. 2005; 73:4451–4453. [PubMed: 15972548]

[23]. Iwaki T, Castellino FJ. A single plasmid transfection that offers a significant advantage associated with puromycin selection in *Drosophila* Schneider S2 cells expressing heterologous proteins. Cytotechnology. 2008; 57:45–49. [PubMed: 19003171]

[24]. Lee J, Lee H-J, Shin M-K, Ryu W-S. Versatile PCR-mediated insertion or deletion mutagenesis. Biotechniques. 2004; 36:398–400. [PubMed: 15038153]

[25]. Wang SG, Reed GL, Hedstrom L. Zymogen activation in the streptokinase–plasminogen complex – ile1 is required for the formation of a functional active site. Eur. J. Biochem. 2000; 267:3994–4001. [PubMed: 10866798]

[26]. Violand BN, Byrne R, Castellino FJ. The effect of a-w-amino acids on human plasminogen structure and activation. J. Biol. Chem. 1978; 253:5395–5401. [PubMed: 670204]

[27]. Urano T, Chibber BAK, Castellino FJ. The reciprocal effects of eaminohexanoic acid and chloride ion on the activation of human [Glu^1]plasminogen by human urokinase. Proc. Natl. Acad. Sci. USA. 1987; 84:4031–4034. [PubMed: 3473492]

[28]. Chibber BAK, Radek JT, Morris JP, Castellino FJ. Rapid formation of an anion sensitive active site in stoichiometric complexes of streptokinase and human [glu^1]plasminogen. Proc. Natl. Acad. Sci. USA. 1986; 83:1237–1241. [PubMed: 3456584]

[29]. McArthur JD, et al. Allelic variants of streptokinase from *Streptococcus pyogenes* display functional differences in plasminogen activation. FASEB J. 2008; 22:3146–3153. [PubMed: 18511548]

[30]. Wang XQ, Lin XL, Loy JA, Tang J, Zhang XJC. Crystal structure of the catalytic domain of human plasmin complexed with streptokinase. Science. 1998; 281:1662–1665. [PubMed: 9733510]

[31]. Conejero-Lara F, Parrado J, Azuaga AI, Smith RAG, Ponting CP, Dobson CM. Thermal stability of the three domains of streptokinase studied by circular dichroism and nuclear magnetic resonance. Protein Sci. 1996; 5:2583–2591. [PubMed: 8976567]

[32]. McShan WM, et al. Genome sequence of a nephritogenic and highly transformable M49 strain of Streptococcus pyogenes. J. Bacteriol. 2008; 190:7773–7785. [PubMed: 18820018]

[33]. Larkin MA, et al. Clustal W and Clustal X version 2.0. Bioinformatics. 2007; 23:2947–2948. [PubMed: 17846036]

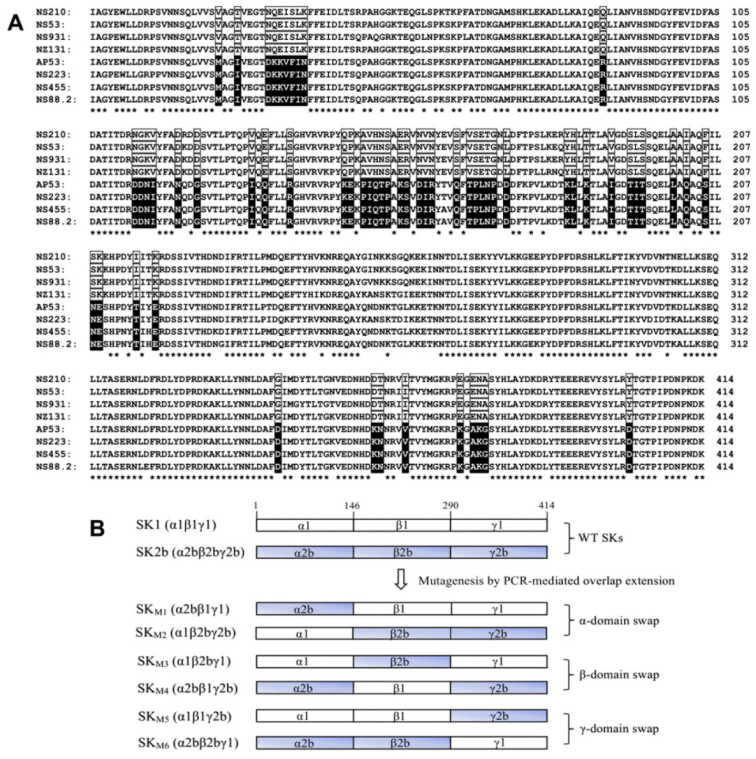

Fig. 1.

Structures of the proteins employed. (A). Sequence alignments of SK and SK2b from various GAS strains. Shown are amino-acid sequences of four SK1s (SK_{NS210}, SK_{NS53}, SK_{NS931}, SK_{NZ131}) and four SK2bs (SK_{AP53}, SK_{NS223}, SK_{NS455} and $SK_{NS88.2}$) [21,32]. Strictly conserved residues in all SK1s and SK2bs are indicated with asterisks. The residues that are strictly conserved in one cluster, and different between clusters, are boxed (clear boxed for SK1, black boxed for SK2b). The sequence alignments were performed with ClustalX [33]. (B). Diagrams of the α, β, and γ domain-exchanged SK mutants from SK1 (NS931) and SK2b (NS88.2) used in this study. Domains were assigned according to the crystal structure of SKg [30].

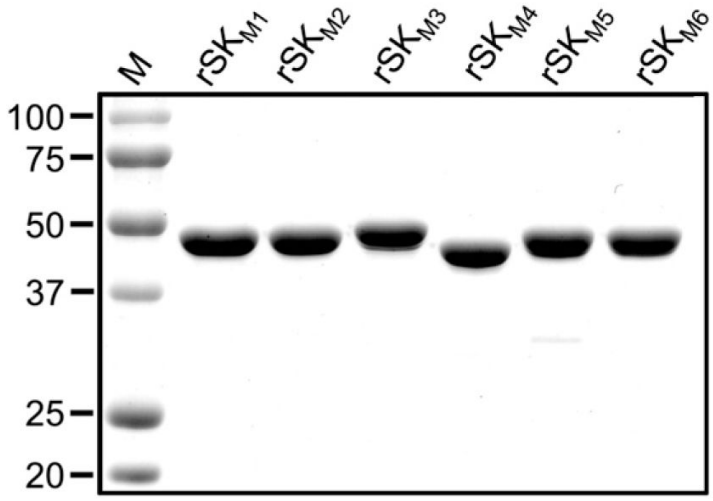

Fig. 2.
SDS–polyacrylamide gels showing the rSK mutants purified in this study.

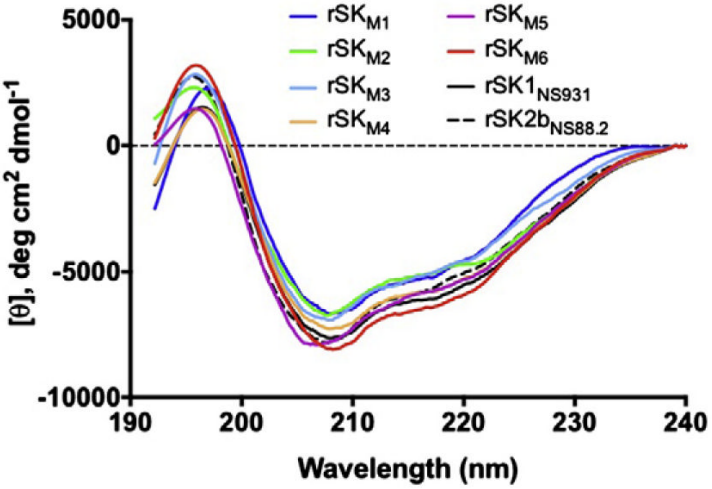

Fig. 3.

Far-UV CD spectra of the purified domain-exchanged SK mutants. Each curve is an average of 3 scans/protein (2 μM) in 10 mM sodium phosphate, pH 7.4, 25 °C.

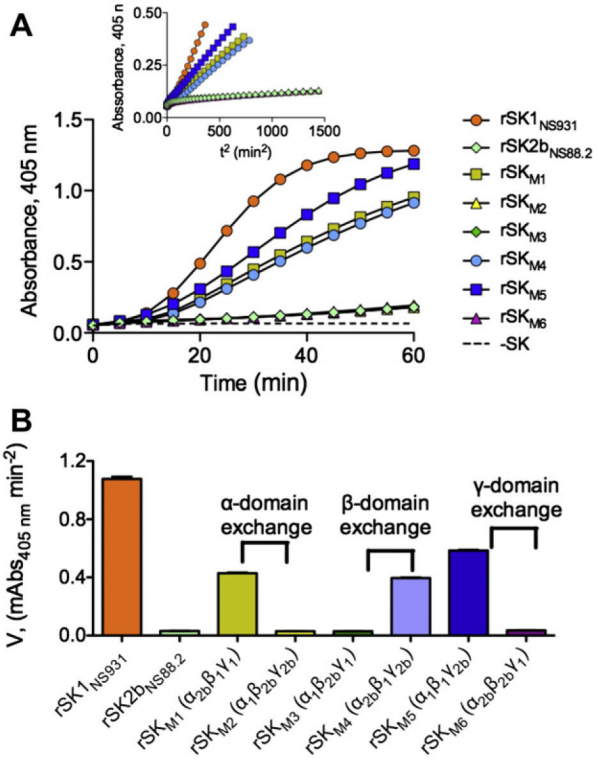

Fig. 4.

Activation of rGlu[1]-hPg by purified domain-exchanged SK mutants. (A). The rate of development of amidolytic activity monitored continuously by the absorbance at 405 nm at 37 °C using the chromogenic hPm substrate, S2251 (H-D-Val-Leu-Lys-pNA·2HCl). The control without rSK (dashed line) was performed under the same conditions. The inset shows the transformed plot of Absorbance at 405 nm *vs.* t^2. (B). The initial velocities of hPm appearance for each rSK variant as calculated by linear regression from the linear regions of plots A_{405} nm *vs.* t^2.

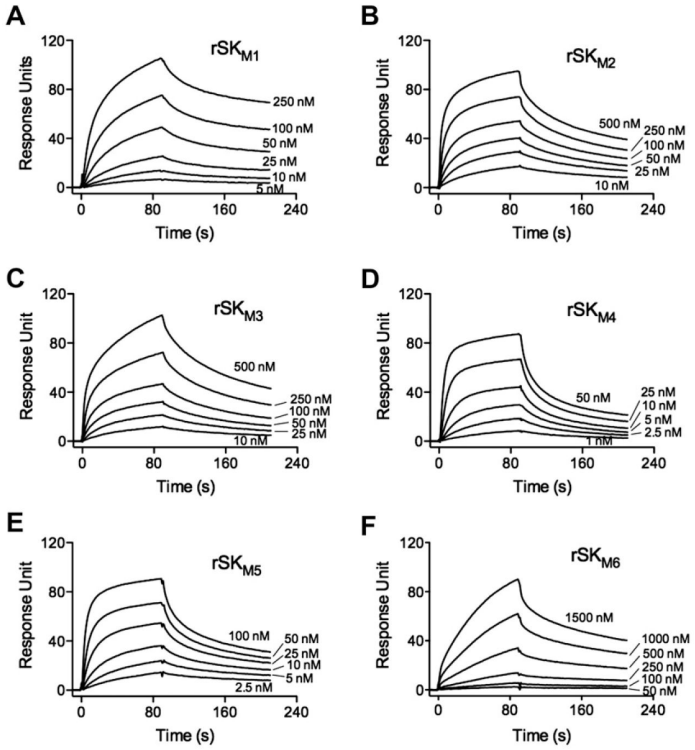

Fig. 5.

Binding of rSKs to rGlu^{1}-hPg[S^{741}A]. SPR sensorgrams for rSK$_{M1}$–rSK$_{M6}$ are illustrated. The curves in each panel represent the binding of the indicated concentrations of the rSKs to rGlu^{1}-hPg[S^{741}A] immobilized on a CM5 chip. The sensorgrams shown were generated by subtraction of the nonspecific refractive index component from the total binding. The CM5 chips were coupled with 1000 RU of rGlu1-hPg[S^{741}A]. To calculate the K_d for each of these SK variants, the protein concentration ranges were: rSK$_{M1}$, 5–250 nM; rSK$_{M2}$ and rSK$_{M3}$, 10–500 nM; rSK$_{M4}$, 1–50 nM; rSK$_{M5}$, 2.5–100 nM; and rSK$_{M6}$, 50–1500 nM. Sensorgrams for the WT-rSK1$_{NS931}$ and WT-rSK2b$_{NS88.2}$ are shown in Ref. [21].

Table 1

K_d values of rSK variants to hPg [$S^{741}A$].

Protein	Domains	K_d (nM)
WT-rSK_{NS931}[a]	$\alpha_1 \beta_1 \gamma_1$	12
WT-$rSK_{NS88.2}$[a]	$\alpha_{2b} \beta_{2b} \gamma_{2b}$	202
rSK_{M1}	$\alpha_{2b} \beta_1 \gamma_1$	24
rSK_{M2}	$\alpha_1 \beta_{2b} \gamma_{2b}$	74
rSK_{M3}	$\alpha_1 \beta_{2b} \gamma_1$	121
rSK_{M4}	$\alpha_{2b} \beta_1 \gamma_{2b}$	11
rSK_{M5}	$\alpha_1 \beta_1 \gamma_{2b}$	19
rSK_{M6}	$\alpha_{2b} \beta_{2b} \gamma_1$	253

[a]Values taken from [21].